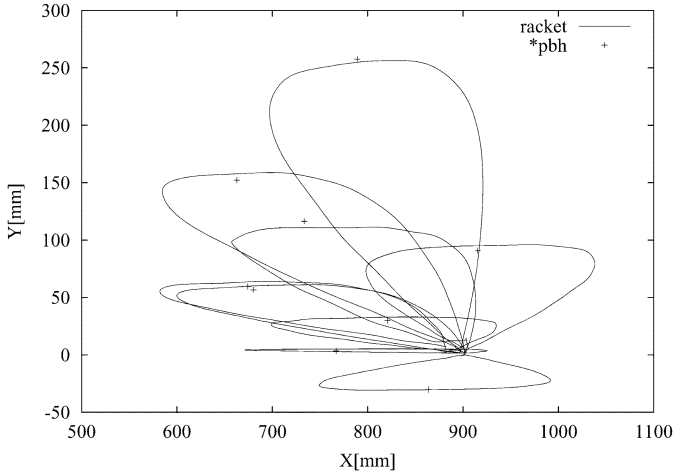

Fig. 12. Paddle trajectory x in the "rally task."

we can see that a given stroke movement of the paddle is accurately achieved by the input determined using the proposed method.

VI. Experimental Results

A. Experimental Results of the "Ball Controlling Task"

We evaluated the capability of controlling the flight duration of the returned ball with the acquired maps. We fixed the desired landing point as $x = -1100$ [millimeters], $y = 300$ [millimeters] and set the desired flight duration as 0.5 [seconds] and 0.7 [seconds], alternatively. We can see from Figs. 8 and 9 that the robot achieves the different ball trajectory with the same landing position by controlling the flight duration.

B. Experimental Results of the Rally Task With a Human

We also demonstrate the robot rally with a human (Fig. 10). The "rally task" means the table tennis rally that people generally play. We consider it as the repetition of "ball controlling task" described above. In the experiment, a human hit a ball toward the robot at random and the robot returned the ball with a fixed duration of flight ($dt_{hr} = 0.55$ [seconds]) to a desired landing point ($p_{rx} = 1550$ [millimeters], $p_{ry} = 0.3 \times {}^{*}p_{bhy}$) for the opponent's easy hitting, where ${}^{*}p_{bhy}$ is a predicted impact point.

Figs. 11 and 12 show a part of the ball and paddle trajectories on the x–y plane in the rally where the waiting position of the paddle is $x = 900$ [millimeters], $y = 0$ [millimeters]. We can see that the robot returns the ball to the point the opponent can hit easily by changing the impact point back and forward, right and left. You can see a short movie of "rally task experiment" at http://robotics.me.es.osaka-u.ac.jp/MiyazakiLab/ Research/ping-pong/.

VII. Conclusion

We have described an approach for a robot to perform the table tennis task based on two kinds of memory-based learning, one of which accurately achieves the stroke movement of the paddle and the other of which determines the paddle conditions at the impact point so as to return the ball to a desired landing point with a specified flight duration. Experimental results including rallies with a human opponent also have been reported.

References

[1] R. R. Burridge, A. A. Rizzi, and D. E. Koditschek, "Sequential composition of dynamically dextrous robot behaviors," *Int. J. Robot. Res.*, vol. 18, no. 6, pp. 534–555, 1999.
[2] R. A. Schmidt and T. D. Lee, "Motor control and learning a behavioral emphasis," *Human Kinetics*, to be published.
[3] R. L. Andersson, *A Robot Ping-Pong Player: Experiment in Real-Time Intelligent Control*. Cambridge, MA: MIT Press, 1988.
[4] M. Ramanantsoa and A. Duray, "Toward a stroke construction model," *Int. J. Table Tennis Sci.*, no. 2, pp. 97–114, 1994.
[5] F. Miyazaki, M. Takeuchi, M. Matsushima, T. Kusano, and T. Hashimoto, "Realization of table tennis task based on virtual targets," in *Proc. IEEE Int. Conf. Robotics and Automation (ICRA)*, Washington, DC, 2002, pp. 3844–3849.
[6] M. Bühler, D. E. Koditschek, and P. J. Kindlmann, "Planning and control of a juggling robot," *Int. J. Robot. Res.*, vol. 13, no. 2, pp. 101–118, 1994.
[7] C. G. Atkeson, A. W. Moore, and S. Schaal, "Locally weighted learning," *Artif. Intell. Rev.*, vol. 11, pp. 11–73, 1997.
[8] S. Arimoto, S. Kawamura, and F. Miyazaki, "Bettering operation of robots by learning," *J. Robot. Syst.*, vol. 1, no. 2, pp. 123–140, 1984.

The Effects of Partial Observability When Building Fully Correlated Maps

Juan Andrade-Cetto and Alberto Sanfeliu

***Abstract*—This paper presents an analysis of the fully correlated approach to the simultaneous localization and map building (SLAM) problem from a control systems theory point of view, both for linear and nonlinear vehicle models. We show how partial observability hinders full reconstructibility of the state space, making the final map estimate dependent on the initial observations. Nevertheless, marginal filter stability guarantees convergence of the state error covariance to a positive semidefinite covariance matrix. By characterizing the form of the total Fisher information, we are able to determine the unobservable state space directions. Moreover, we give a closed-form expression that links the amount of reconstruction error to the number of landmarks used. The analysis allows the formulation of measurement models that make SLAM observable.**

***Index Terms*—Estimation, localization, mapping, mobile robots, simultaneous localization and map building (SLAM).**

I. Introduction

The study of stochastic models for simultaneous localization and map building (SLAM) in mobile robotics has been an active research topic for over 15 years. One of the main difficulties in providing a robust solution to the SLAM problem resides in the fact that it is a fully correlated state estimation problem. That is, the state space constructed by appending the robot pose and the landmark locations is fully correlated, which is a situation that produces partial observability. Moreover, the modeling of map states as static landmarks yields a partially controllable state vector.

The study of fully correlated estimation due to geometric constraints was originally addressed by Durrant-Whyte [1]. Within the Kalman filter (KF) approach to SLAM, seminal work by Smith and Cheeseman [2] suggested that, as successive landmark observations take place, the

Manuscript received September 9, 2003; revised April 6, 2004 and October 10, 2004. This paper was recommended for publication by Associate Editor W. Chung and Editor S. Hutchinson upon evaluation of the reviewers' comments. This work was supported by the Spanish Council of Science and Technology under Project DPI-2001-2223.

The authors are with the Institut de Robòtica i Informàtica Industrial, 08028 Barcelona, Spain (e-mail: cetto@iri.upc.es).

Digital Object Identifier 10.1109/TRO.2004.842342

correlation between the estimates of the location of such landmarks in a map grows continuously. This observation was ratified by Dissanayake *et al.* [3] with a proof showing that the estimated map converges monotonically to a relative map with zero uncertainty. They also showed how the absolute accuracy of the map reaches a lower bound defined only by the initial vehicle uncertainty and proved it for a one-landmark vehicle with no process noise.

In the KF approach to SLAM, neither the vehicle nor the landmarks are ever precisely reconstructed and thus the need to maintain all of the vehicle-to-landmark and landmark-to-landmark correlations. This situation poses a scaling problem, and current efforts in SLAM are tailored at tackling it by estimating a map of relations, in which the absolute vehicle estimate is not part of the state vector [4], by maintaining an interconnected set of local coordinate frames, or by decorrelating state estimates via covariance inflation [5], among other solutions.

Explicit solutions to the continuous time SLAM problem for a one-dimensional (1-D) vehicle were presented by Gibbens *et al.* [6] and Kim [7]. Both works give closed-form expressions for the asymptotic value of the state error covariance $\mathbf{P}$. Kim observed that, for the case when not all landmarks are observed at all times, the asymptotic value on the determinant of $\mathbf{P}$ reaches a constant value greater than zero. Gibbens *et al.*, on the other hand, observed that the rate of convergence of $\mathbf{P}$ is proportional to the number of landmarks used n, in the form of the total Fisher information $I_T = \sum_1^n \sigma_w^{-2}$ per unit time (with σ_w^2 the sensor variance). Moreover, they show that the asymptotic value of $\mathbf{P}$ is independent of the plant variance. The expression used for I_T is derived from a simple likelihood function, one that does not contain the fully correlated characteristics of the measurement model. In Section II, we derive a new expression for the total Fisher information in SLAM, from the maximization of a likelihood function at the value of the state $\mathbf{x}$ that most likely gave rise to the observed data Z^k. The analysis yields a closed-form solution that shows, explicitly, the unobservable directions of the map state.

In Section III, we show that the filter typically used in SLAM is marginally stable; in general, which is an undesirable feature in state estimation, making the final steady state of the filter dependent on the initial noise parameters, but guaranteeing the existence of at least one *psd* solution to the Riccati equation for the steady-state covariance.

General expressions for the controllable and observable subspaces in SLAM are derived in Section IV and later simplified in Sections V and VI for a 1-D vehicle (*the monobot*), and for a planar wheeled vehicle, respectively. We prove, in the end, that the angle between these two subspaces is determined only by the total number of landmarks in the map. The result is that, as the number of landmarks increases, the state components get closer to being reconstructible. We show experimentally that the average error in state estimation is proportional to the number of landmarks used.

Partial observability makes impossible a full reconstruction of the map state vector, with typical measurement models, regardless of the vehicle model chosen. In Section VII, we show how partial observability in SLAM can be avoided by adding a fixed external sensor to the state model or, equivalently, by setting a fixed landmark in the environment to serve as global localization reference. Full observability guarantees a steady flow of the information about each state component and prevents the uncertainty (error state covariance) from becoming unbounded if, for example, covariance inflation is to be used in the quest for decorrelation [8].

II. Total Fisher Information

Under the Gaussian assumption for the vehicle and sensor noises, the KF is the optimal minimum mean-square error estimator. Also, minimizing the least-squares (LS) criteria $E[\tilde{\mathbf{x}}_k \tilde{\mathbf{x}}_k^\top | Z^k]$, is equivalent to the maximization of a likelihood function $\Lambda(\mathbf{x})$ given the set of observations Z^k, that is, the maximization of the joint probability density function (pdf) of the entire history of observations [9]

$$\Lambda(\mathbf{x}) = \prod_{i=1}^{k} p(\mathbf{z}_i | \mathbf{x}, Z^{i-1}) \tag{1}$$

where $\mathbf{x}$ is the augmented map state (vehicle and landmark estimates), and $\mathbf{z}_i$ is the entire observation vector at time i. Given that the above pdfs are Gaussian, and that $E[\mathbf{z}_i] = \mathbf{H}\mathbf{x}_{i|i-1}$, the pdf for each measurement in SLAM is $p(\mathbf{z}_i | Z^{i-1}) = N(\tilde{\mathbf{z}}_{i|i-1}; \mathbf{0}, \mathbf{S}_i)$, where $\mathbf{H}$ is the observation matrix, and $\mathbf{S}_i = E[\tilde{\mathbf{z}}_{i|i-1} \tilde{\mathbf{z}}_{i|i-1}^\top]$ is the innovation covariance.

In practice, however, it is more convenient to consider the log-likelihood function $\ln \Lambda(\mathbf{x})$. The maximum of $\ln \Lambda(\mathbf{x})$ is at the value of the state $\mathbf{x}$ that most likely gave rise to the observed data Z^k and is obtained by setting its derivative with respect to $\mathbf{x}$ equal to zero, which gives

$$\nabla_{\mathbf{x}} \ln \Lambda(\mathbf{x}) = \sum_{i=1}^{k} \mathbf{H}^\top \mathbf{S}_i^{-1} \tilde{\mathbf{z}}_{i|i-1}. \tag{2}$$

An intuitive interpretation of the maximum of the log-likelihood is that the best estimate for the state $\mathbf{x}$, in the LS sense, is the one that makes the sum of the entire set of Mahalanobis distances $\sum_{i=1}^{k} \tilde{\mathbf{z}}_{i|i-1}^\top \mathbf{S}_i^{-1} \tilde{\mathbf{z}}_{i|i-1}$ as small as possible, which is a measure that is consistent with the spatial compatibility test described in [10].

Let $\mathbf{P}_{r,0|0}$, $\mathbf{Q}$, and $\mathbf{R}$ denote the initial vehicle, plant, and sensor covariances, respectively. The Fisher information matrix, a quantification of the maximum existing information in the observations about the state $\mathbf{x}$, is defined as the expectation on the dyad of the gradient of $\ln \Lambda(\mathbf{x})$, that is, $\mathbf{J} = E[(\nabla_{\mathbf{x}} \ln \Lambda(\mathbf{x}))(\nabla_{\mathbf{x}} \ln \Lambda(\mathbf{x}))^\top]$. Taking the expectation on the innovation error in the preceding equation gives the sum

$$\mathbf{J} = \sum_{i=1}^{k} \mathbf{H}^\top (\mathbf{H}\mathbf{P}\mathbf{H}^\top + \mathbf{R})^{-1} \mathbf{H}. \tag{3}$$

It is easy to verify that, in the linear case, this expression for the total Fisher information is only a function of $\mathbf{P}_{r,0|0}$, $\mathbf{Q}$, and $\mathbf{R}$. If, on the other hand, the EKF is used, the Jacobian $\mathbf{H}$ in (3) should be evaluated at the true value of the states $\mathbf{x}_0, \ldots \mathbf{x}_k$. Since these are not available, an approximation is obtained at the estimates $\mathbf{x}_{i|i-1}$. The pre- and post-multiplying $\mathbf{H}$ is, in this context, also known as the *sensitivity matrix*.

A necessary condition for the estimator (the KF) to be consistent in the mean-square sense is that there must be an increasing amount of information about the state $\mathbf{x}$ in the measurements. That is, as $k \to \infty$, the Fisher information must also tend to infinity. Note how, as the total number of landmarks grows, the total Fisher information also grows, directly relating the number of landmarks to the amount of information available for state estimation in SLAM.

Solving for the kth sum term in $\mathbf{J}$ for the monobot (a 1-D vehicle with landmarks located along the mere axis of motion)

$$\mathbf{J}_k = \begin{bmatrix} \sum\sum \varsigma_{ij} & -\boldsymbol{\varsigma} \\ -\boldsymbol{\varsigma}^\top & \mathbf{S}_k^{-1} \end{bmatrix} \tag{4}$$

where ς_{ij} is the ijth entry in $\mathbf{S}_k^{-1}$, and $\boldsymbol{\varsigma} = [\sum \varsigma_{1i}, \ldots, \sum \varsigma_{ni}]$. Unfortunately, it can be easily shown, at least for the monobot case, that the first row (or column) of $\mathbf{J}$ is equivalent to the sum of the rest of the rows (or columns), producing a singular total Fisher information matrix. Citing Bar-Shalom *et al.* [9]: "*a singular Fisher information matrix means total uncertainty in a subspace of the state space, that is, the information is insufficient for the estimation problem at hand.*" SLAM is unobservable. This is a consequence of the form of the Jacobian $\mathbf{H}$, i.e., of the full correlation in SLAM. Zero eigenvalues of $\mathbf{H}^\top \mathbf{S}^{-1} \mathbf{H}$

are an indicator of partial observability, and the corresponding eigenvectors give the unobservable directions in state space.

So, for example, for a one-landmark monobot, the innovation variance is the scalar $s = \sigma_r^2 - 2\rho_{rf}\sigma_r\sigma_f + \sigma_f^2 + \sigma_w^2$, and, since $\mathbf{H} = [-1, 1]$, the Fisher information matrix in (3) evaluates to

$$\mathbf{J} = \begin{bmatrix} 1 & -1 \\ -1 & 1 \end{bmatrix} \sum_{i=1}^{k} \frac{1}{s_i}. \tag{5}$$

The unobservable direction of the state space is the eigenvector associated with the null eigenvalue of $\mathbf{J}$; we denote it for now as $\mathbf{E}_{\mathrm{Ker}\mathcal{O}}$ (the name will be clear soon) and it evaluates to

$$\mathbf{E}_{\mathrm{Ker}\mathcal{O}} = \begin{pmatrix} 1 \\ 1 \end{pmatrix}. \tag{6}$$

III. Steady-State Behavior of SLAM

Let the linearized SLAM state model be

$$\mathbf{x}_{k+1} = \mathbf{F}\mathbf{x}_k + \mathbf{G}\mathbf{v}_k \tag{7a}$$

$$\mathbf{z}_{k+1} = \mathbf{H}\mathbf{x}_{k+1} + \mathbf{w}_{k+1}. \tag{7b}$$

Moreover, let $\mathbf{K}$ be the Kalman gain matrix. In SLAM, the matrix $\mathbf{F} - \mathbf{KH}$ is semistable, i.e., it has a unit circle eigenvalue [11]. Thus, the one-step-ahead form of the prediction for the error state dynamics

$$\tilde{\mathbf{x}}_{k+1|k} = (\mathbf{F} - \mathbf{KH})\tilde{\mathbf{x}}_{k|k-1} + \mathbf{G}\mathbf{v}_k - \mathbf{K}\mathbf{w}_k \tag{8}$$

is bounded in the steady state by a constant value, subject to the filter initial conditions.

The steady-state error covariance matrix is given by the solution of the one-step-ahead Riccati equation

$$\mathbf{P} = (\mathbf{F} - \mathbf{KH})\mathbf{P}(\mathbf{F} - \mathbf{KH})^\top + \mathbf{G}\mathbf{Q}\mathbf{G}^\top + \mathbf{K}\mathbf{H}\mathbf{R}\mathbf{H}^\top\mathbf{K}^\top \tag{9}$$

which, by the same reason, converges at least to one psd solution. For the linear case, the solution of (9) is a function of $\mathbf{P}_{r,0|0}, \mathbf{Q}, \mathbf{R}$ and the total number of landmarks n. Note, however that, for the nonlinear case, the computation of the Jacobians $\mathbf{F}$ and $\mathbf{H}$ will in general also depend on the steady-state value of $\mathbf{x}$.

For a linear robot with perfect data association and constant vehicle and sensor variances, the computation of $\mathbf{K} = \mathbf{P}\mathbf{H}^\top(\mathbf{H}\mathbf{P}\mathbf{H}^\top + \mathbf{R})^{-1}$ could be performed offline. That is, the asymptotic behavior of $\mathbf{P}$ and its rate of convergence are always the same, regardless of the actual motions and measurements.

IV. Controllable and Observable Subspaces

To see what part of the state space is compromised by full correlation, we now develop closed-form expressions for the bases of the controllable and observable subspaces in SLAM and relate them to the total number of landmarks used. The controllability matrix for the plant in 7(a)–(b) is

$$\mathcal{C} = [\mathbf{G} \quad \mathbf{F}\mathbf{G} \quad \dots \quad \mathbf{F}^{\dim \mathbf{x}-1}\mathbf{G}]. \tag{10}$$

The dimensionality of the controllable subspace, spanned by the column space of $\mathcal{C}$, is $\mathrm{rank}\mathcal{C} = \dim \mathbf{x}_r$, regardless of the number of landmarks in the map. Obviously, the only controllable states are the ones associated with the vehicle motion. The observability matrix of our system becomes

$$\mathcal{O} = \begin{bmatrix} \mathbf{H} \\ \mathbf{H}\mathbf{F} \\ \vdots \\ \mathbf{H}\mathbf{F}^{\dim \mathbf{x}-1} \end{bmatrix}. \tag{11}$$

The rank of $\mathcal{O}$ indicates the dimensionality of the observable subspace, which, in turn, is spanned by the row space of $\mathcal{O}$. $\mathrm{rank}\mathcal{O} = \dim \mathbf{x} - \dim \mathbf{x}_f^{(i)}$, with $\mathbf{x}_f^{(i)}$ any landmark in $\mathbf{x}$. That is, all but one landmark size of the state vector $\mathbf{x}$ is reconstructible.

V. Relationship Between Subspaces: The Monobot

Consider the case of the one-landmark monobot. By substituting the resulting expressions for the model Jacobians, the controllability and observability matrices reduce to

$$\mathcal{C} = \begin{bmatrix} 1 & 1 \\ 0 & 0 \end{bmatrix}, \quad \mathcal{O} = \begin{bmatrix} -1 & 1 \\ -1 & 1 \end{bmatrix}. \tag{12}$$

The controllable subspace has a basis of the form $(q, 0)^\top$, clearly indicating that the only dimension in the state space that can be controlled is the one associated with the motion of the robot. The observable subspace on the other hand, with basis $(r, -r)^\top$, shows how the observed robot and landmark locations are fully correlated. The unobservable subspace is the orthogonal complement of $\mathrm{Im}\mathcal{O}^\top$ and has a basis $(r, r)^\top$. An expression for it was already derived from the analysis of the total Fisher information matrix and is given in (6). The name $\mathbf{E}_{\mathrm{Ker}\mathcal{O}}$ indicates that it is a basis for the null space of $\mathcal{O}$.

A measure of the error incurred while trying to reconstruct the state $\mathbf{x}$ from correlated observations is given by the angle between these two subspaces. For the one landmark monobot, the angle is $\alpha = \angle \mathrm{Im}\mathcal{C}\mathrm{Im}\mathcal{O}^\top = \pi/4$. The angle α indicates how close noise-driven observations are from fully revising the robot part of the state space.

What happens if we add more landmarks to the environment? Will the vehicle and landmark location estimates improve or degrade? Will we be able to achieve an uncoupled reconstruction of the entire state space? The answer to the above questions is "improve" but "no."

Consider the two-landmark monobot case. A possible set of bases for the controllable and observable subspaces are

$$\mathbf{E}_{\mathrm{Im}\mathcal{C}} = \begin{pmatrix} 1 \\ 0 \\ 0 \end{pmatrix}, \quad \mathbf{E}_{\mathrm{Im}\mathcal{O}^\top} = \begin{pmatrix} 1 & 1 \\ -1 & 0 \\ 0 & -1 \end{pmatrix} \tag{13}$$

and the angle between these two subspaces can be computed as the smallest nonnull singular value of the product of their orthonormal bases. $\alpha = \angle \mathrm{Im}\mathcal{C}\mathrm{Im}\mathcal{O}^\top = 163\pi/832$. Following this procedure, we computed the value of α for a three-landmark monobot model, further reducing to $\alpha = \pi/6$. Also, as we add more landmarks to the map, the angle between the observable and controllable subspaces reduces monotonically. Fig. 1(a) shows experimentally the decrease in α as landmarks are added to the map. Such monotonic reduction in α suggests that our measurement noise-driven corrections to the map state estimate would reconstruct the vehicle localization estimate closer to the actual value of the vehicle pose.

Theorem 1: In the case of a linear 1-D robot, the angle between the controllable and observable subspaces in the KF-SLAM algorithm depends only on the total number of landmarks used n and is given by $\alpha = \arccos\sqrt{n/(n+1)}$.

Proof: Generalizing (13) to the n-landmark case, a set of possible bases for the controllable and observable subspaces are given by $\mathbf{E}_{\mathrm{Im}\mathcal{C}} = [\mathbf{q}] = \begin{pmatrix} 1 \\ \mathbf{0}_{n\times 1} \end{pmatrix}$, and $\mathbf{E}_{\mathrm{Im}\mathcal{O}^\top} = [\mathbf{r}_1 \ \dots \ \mathbf{r}_n] = \begin{pmatrix} \mathbf{1}_{1\times n} \\ -\mathbf{I} \end{pmatrix}$, respectively. Let $\mathbf{p}$ be the projection of $\mathbf{E}_{\mathrm{Im}\mathcal{C}}$ onto $\mathbf{E}_{\mathrm{Im}\mathcal{O}^\top}$. $\mathbf{p}$ is easily computed as the sum of the individual projections of $\mathbf{q}$ onto each element $\mathbf{r}_i$ of the basis of the observable subspace, i.e., $\mathbf{p} = \sum_{i=1}^{n} (\mathbf{q}^\top\mathbf{r}_i)/(\mathbf{r}_i^\top\mathbf{r}_i)\mathbf{r}_i$ Substituting the basis of the controllable subspace gives the reduced expression

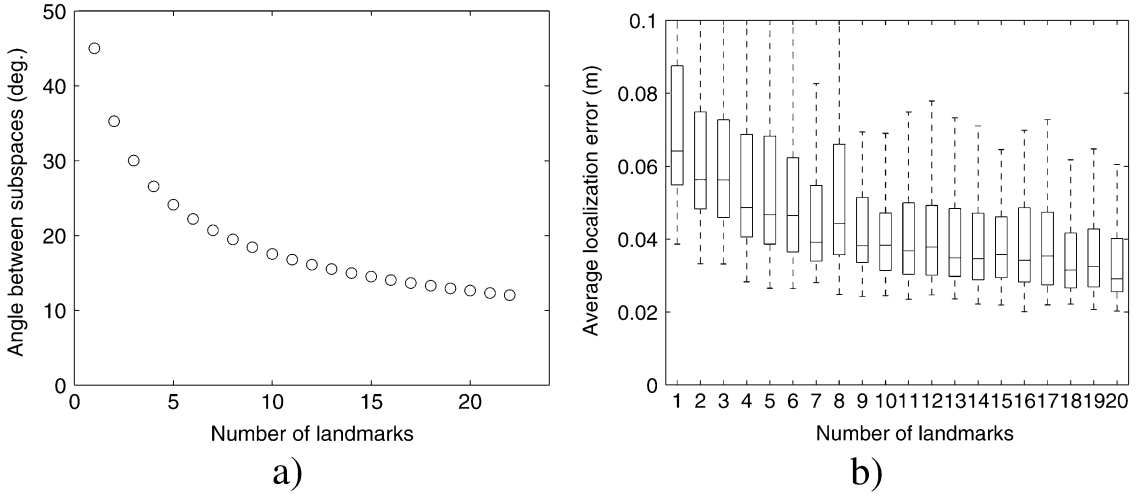

Fig. 1. (a) $\angle \mathrm{Im}\mathcal{C}\mathrm{Im}\mathcal{O}^\top$. Angle between the observable and controllable subspaces. (b) Reduction of the average monobot localization error $\mathbf{x}_{r,k} - \mathbf{x}_{r,k|k}$ with respect to the number of landmarks used. The results correspond to a Monte Carlo simulation over 100 SLAM runs. The dotted lines show the extent of the data for the entire set of runs, and the boxes contain marks at the lower, median, and upper quartiles.

$\mathbf{p} = (1/2)\sum_{i=1}^{n} \mathbf{r}_i = (1/2)\begin{bmatrix} n \\ -\mathbf{1}_{n\times 1} \end{bmatrix}$ Finally, the angle between $\mathbf{p}$ and $\mathbf{q}$, and consequently between the two subspaces, is $\alpha = \arccos(\mathbf{p}^\top \mathbf{q})/(\|\mathbf{p}\|\|\mathbf{q}\|) = \arccos\sqrt{n/(n+1)}$. ■

As the number of landmarks grows, the observable subspace gets closer to the controllable part of the state space (the vehicle localization states). $\lim_{n\to\infty} \alpha = 0$. It is unrealistic, however, to have an infinite number of landmarks, and a compromise has to be made between the possibility of including as many landmarks as possible and the amount of information that new observations give. Also, one has to bear in mind that, as more and more landmarks are added to the map, their associated measurement noise is also added.

It has been argued that the performance of any SLAM algorithm would be enhanced by concentrating on fewer, better landmark observations [6]. That is certainly true, as little gain (little reduction in α) is attained when going from 25 to 125 landmarks compared to the move from 1 to 5 or 5 to 25.

In Fig. 2, we have plotted the results of using the original fully correlated KF approach to SLAM for a monobot that starts at location $\mathbf{x}_{r,0|0} = -1m$ and moves along a straight line with a temporal sinusoid trajectory returning to the same point after 100 iterations. Landmarks are located at $\mathbf{x}_{f(i)} = 1m$. A plant noise model proportional to the motion command and a measurement noise model proportional to the distance from the sensor to the landmark are used. The dotted lines indicate 2σ bounds on the state estimates.

The effects of partial observability manifest the dependence on the initial conditions. Note how both the vehicle and landmark mean localization errors do not converge to zero. Their steady-state value is subject to the error incurred at the first observation. That is, the filter is marginally stable (the matrix $\mathbf{F} - \mathbf{KHF}$ has a pole in one [11]).

However, a Monte Carlo simulation over 100 SLAM runs showed filter unbiasedness, which is a property of optimal stochastic state estimation (KF). That is, the average landmark localization error over the entire set of simulations was still zero, thanks to the independence of the initial landmark measurement errors at each test run.

The steady-state error for the robot and landmark localization is less sensitive to the initial conditions when a large number of landmarks are used. The reason is the same as for the Monte Carlo simulation, the observations are independent, and their contribution averages at each iteration in the computation of the localization estimate. The results of the Monte Carlo simulation are shown in Fig. 1(b), depicting the effect of the increase in the number of landmarks on the average vehicle localization error.

VI. Relationship Between Subspaces: Planar Robot

The reconstructibility issues presented for the linear and 1-D robot of the previous section nicely extend when studying more complicated platforms. Consider a planar robot, a nonlinear wheeled vehicle with three degrees of freedom, and an environment consisting of two-dimensional (2-D) point landmarks located on the floor.

The dimensionality of the controllable subspace is $\dim \mathbf{x}_r = 3$, and, for the specific case in which only one landmark is available, a basis for the controllable subspace is simply

$$\mathbf{E}_{\mathrm{Im}\mathcal{C}} = \begin{pmatrix} \mathbf{I} \\ \mathbf{0}_{2\times 3} \end{pmatrix}.$$

The dimensionality of the observable subspace is, for this particular configuration, $\mathrm{rank}\mathcal{O} = 3$. This last result is easily verified with simple symbolic manipulation of the specific expression for the state model in [12]. Possible bases for $\mathrm{Im}\mathcal{O}^\top$ and for the null space of $\mathcal{O}$ (the unobservable subspace) are

$$\mathbf{E}_{\mathrm{Im}\mathcal{O}^\top} = \begin{pmatrix} 1 & 0 & 0 \\ 0 & 1 & 0 \\ 0 & 0 & 1 \\ -1 & 0 & 0 \\ 0 & -1 & 0 \end{pmatrix} \quad \mathbf{E}_{\mathrm{Ker}\mathcal{O}} = \begin{pmatrix} 1 & 0 \\ 0 & 1 \\ 0 & 0 \\ 1 & 0 \\ 0 & 1 \end{pmatrix}.$$

The only independently observable state is the one associated to the robot orientation θ. The other four states, the Cartesian coordinates of the robot, and landmark locations span a space of dimension 2. Even when $\mathrm{Im}\mathcal{C}$ and $\mathrm{Im}\mathcal{O}^\top$ both span $\mathbb{R}^3$, we see that the inequality $\mathrm{Im}\mathcal{C} \neq \mathrm{Im}\mathcal{O}^\top$ still holds, as in the case of the monobot. That is, the observable and controllable subspaces for the one-landmark three-degree–of–freedom robot SLAM problem correspond to different three-dimensional (3-D) subspaces in $\mathbb{R}^5$, and their intersection represents the only fully controllable and observable state, which, for this particular vehicle model, is the robot orientation. Once more, a measure of the reconstruction error incurred when estimating the vehicle pose from correlated observations is given by the angle between these two subspaces.

Resorting again to a singular value decomposition for the computation of a pair of orthonormal bases for $\mathrm{Im}\mathcal{C}$ and $\mathrm{Im}\mathcal{O}^\top$, we have that,

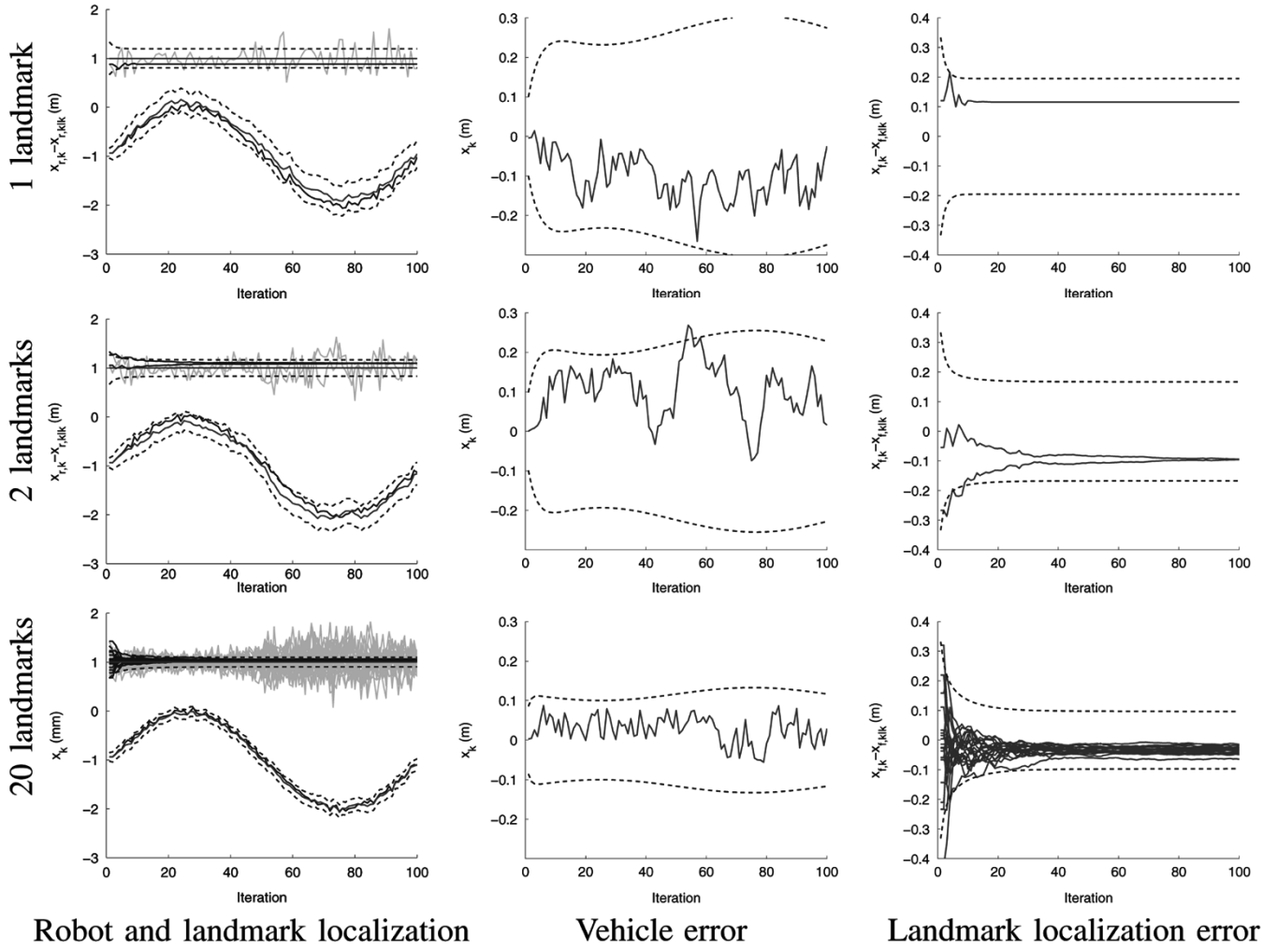

Fig. 2. Full-covariance KF SLAM for a monobot in a sinusoidal path starting at $\mathbf{x}_{r,0|0} = -1$ m, during 100 iterations. The noise-corrupted sinusoidal vehicle trajectory is indicated by the darkest curve in the first column of plots. In the same column, and close to it, is a lighter curve that shows the vehicle location estimate as computed by the filter, along with a pair of dotted lines indicating 2σ bounds on such estimate. The dark straight lines at the 1-m level indicate the landmark location estimates, and the lighter noise corrupted signals represent sensor measurements. Also shown are a pair of dotted lines for 2σ bounds on the landmark location estimates. The second column of plots shows the vehicle localization error and its corresponding covariance, also in the form of 2σ dotted bounds. The last column shows the same for the landmark estimates.

for the one-landmark planar robot case, $\alpha = \pi/4$. For a two-landmark map, $\alpha = 163\pi/832$, for a three-landmark model, $\alpha = \pi/6$, and, as we add more and more landmarks to the environment, the angle between the controllable and observable subspaces reduces monotonically, in exactly the same manner as in the case of the monobot.

Theorem 2: In the case of a nonlinear planar robot with three DOF, the angle between the controllable and observable subspaces in the EKF-SLAM algorithm depends only on the total number of landmarks used n and is given by $\alpha = \arccos\sqrt{n/(n+1)}$.

Proof: Thanks to the orthogonality of the four fundamental subspaces, the angle between the observable and controllable subspaces is exactly the same as the angle between their complementary subspaces. That is, $\alpha = \angle \mathrm{Ker}\mathcal{C}^\top \mathrm{Ker}\mathcal{O}$. The controllable subspace has rank $\dim \mathbf{x}_r = 3$, regardless of the number of landmarks; and the size of the basis for the observable subspace would depend on n. Now the roles are reversed. The dimension of $\mathbf{E}_{\mathrm{Ker}\mathcal{C}^\top}$ grows with respect to the number of landmarks but maintains a very simple form $\mathbf{E}_{\mathrm{Ker}\mathcal{C}^\top} = \begin{bmatrix} \mathbf{0}_{3\times 2n} \\ \mathbf{I} \end{bmatrix}$. The null complement of the observable subspace, on the other hand, has a fixed number of columns (just two), and it can be easily shown by inspection that $\mathbf{E}_{\mathrm{Ker}\mathcal{O}} = [\mathbf{I}\ \mathbf{0}_{2\times 1}\ \mathbf{I}\ \cdots\ \mathbf{I}]^\top_{2\times(3+2n)}$. These are precisely the directions along which our state space is unobservable, clearly showing that, in the EKF-SLAM model, the Cartesian coordinates of the robot and landmark locations are all fully correlated. The angle between these two subspaces is again given by the smallest singular value of an orthonormalized version of the product $\mathbf{E}_{\mathrm{Ker}\mathcal{C}^\top}{}^\top \mathbf{E}_{\mathrm{Ker}\mathcal{O}}$, in which $\mathbf{E}_{\mathrm{Ker}\mathcal{C}^\top} = \mathbf{U}_\mathcal{C}\mathbf{\Sigma}_\mathcal{C}\mathbf{V}_\mathcal{C}^\top$, and $\mathbf{E}_{\mathrm{Ker}\mathcal{O}} = \mathbf{U}_\mathcal{O}\mathbf{\Sigma}_\mathcal{O}\mathbf{V}_\mathcal{O}^\top$. That is, $\mathbf{U}_\mathcal{C}^\top\mathbf{U}_\mathcal{O} = 1/\sqrt{n+1}[\mathbf{I}\ \cdots\ \mathbf{I}]^\top_{2n\times 2}$, and $\alpha = \arccos\sigma_{\min}(\mathbf{U}_\mathcal{C}^\top\mathbf{U}_\mathcal{O}) = \arccos\sqrt{n/(n+1)}$. ■

VII. Full Observability

In Section II, we characterized the unobservable subspace in SLAM as the subspace spanned by the null eigenvectors of the total Fisher information matrix. Furthermore, we showed in Sections IV–VI how the unobservable part of the state space is precisely a linear combination of the landmark and robot pose estimates. In order to gain full observability, we propose to extend the measurement model. We present two techniques to achieve this. One is to let one landmark serve as a fixed global reference, with its localization uncertainty independent of the vehicle pose. The second proposed technique is the addition of a fixed external sensor, such as a camera, a GPS, or a compass, that can measure all or part of the vehicle location state at all times, independent of the landmark estimates. Both techniques are based essentially on the

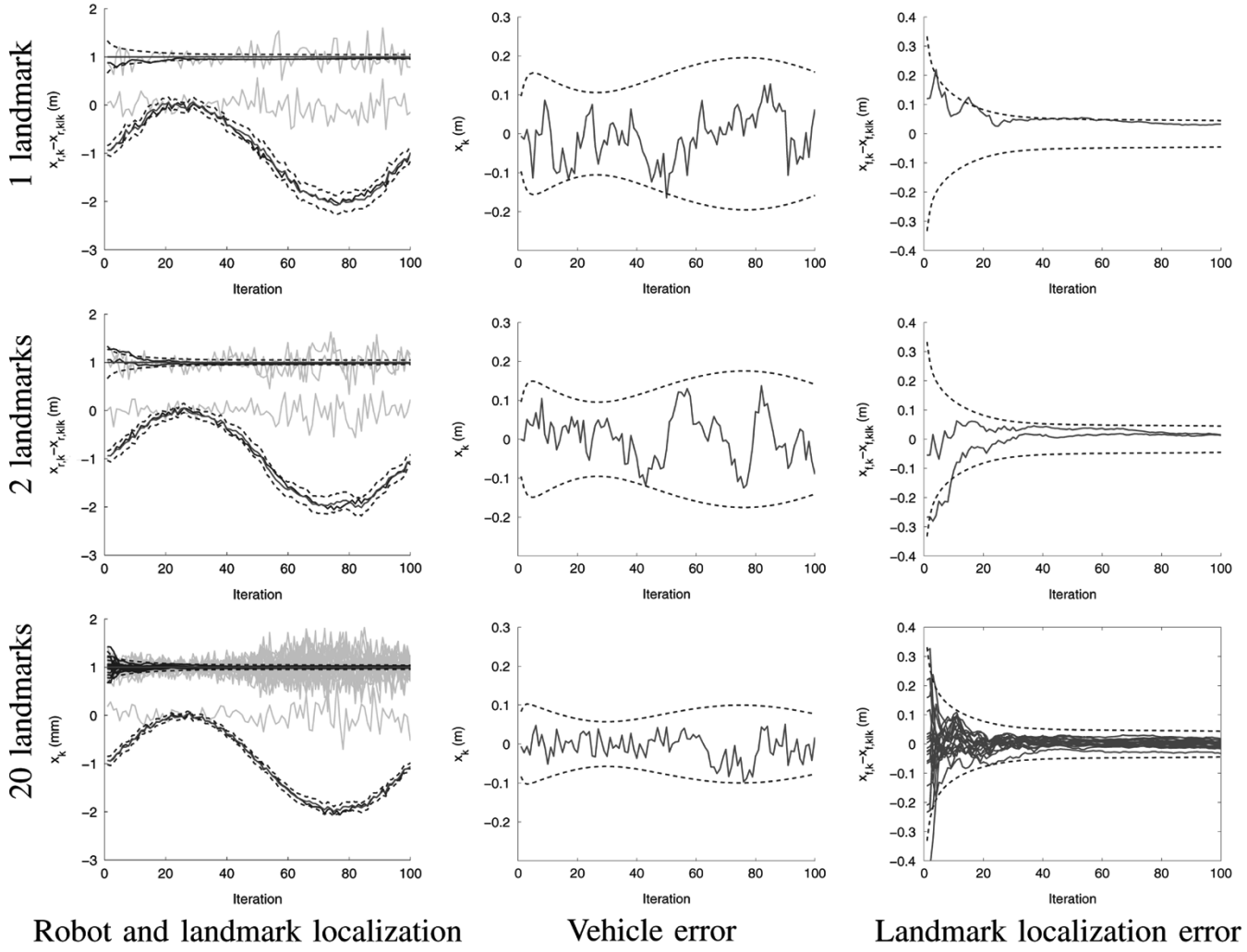

Fig. 3. Full-covariance fully observable KF SLAM for a monobot in a sinusoidal path starting at $\mathbf{x}_{r,0|0} = -1$ m, during 100 iterations. The global reference is located at the origin.

same principle. Full observability requires an uncorrelated measurement Jacobian or, equivalently, a full rank Fisher information matrix.

A. A Fixed Global Reference

The plant model is left untouched, i.e., $\mathbf{x}_{k+1} = \mathbf{x}_k + \mathbf{u}_k + \mathbf{v}_k$, and the measurement model takes now the form

$$\begin{bmatrix} z_k^{(0)} \\ \mathbf{z}_k \end{bmatrix} = \begin{bmatrix} -1 & \mathbf{0}_{1\times n} \\ -\mathbf{1}_{n\times 1} & \mathbf{I} \end{bmatrix} \mathbf{x} + \begin{bmatrix} w_k^{(0)} \\ \mathbf{w}_k \end{bmatrix}. \tag{14}$$

One of the observed landmarks is to be taken as a global reference at the world origin. No map state is needed for it. The zeroth superscript in the measurement vector is used for the consistent indexing of landmarks and observations with respect to the original model. It can be easily shown that the observability matrix for this new model is full rank.

The innovation covariance matrix for the augmented system $\mathbf{S}_{O,k}$ is of size $(n+1)\times(n+1)$, and its inverse can be decomposed in

$$\mathbf{S}_{O,k}^{-1} = \begin{bmatrix} \varsigma_{O,00} & \varsigma_{O,01} & \cdots & \varsigma_{O,0n} \\ \varsigma_{O,01} & & & \\ \vdots & & \hat{\mathbf{S}}_k^{-1} & \\ \varsigma_{O,0n} & & & \end{bmatrix} \tag{15}$$

where $\varsigma_{O,ij}$ is the ijth entry in $\mathbf{S}_{O,k}^{-1}$, $\boldsymbol{\varsigma}_O = [\sum \varsigma_{O,1i}, \ldots, \sum \varsigma_{O,1i}]$, and $\hat{\mathbf{S}}_k^{-1}$ is its submatrix associated with the landmarks that are under estimation (excluding the anchor observation). The kth element of the Fisher information matrix sum in (3) is now

$$\mathbf{J}_{O,k} = \begin{bmatrix} \sum\sum \varsigma_{O,ij} & -\boldsymbol{\varsigma}_O \\ -\boldsymbol{\varsigma}_O^\top & \hat{\mathbf{S}}_k^{-1} \end{bmatrix}. \tag{16}$$

Unlike in (4), this form of the Fisher information matrix is full rank. Moreover, from the properties of positive definite matrices, if $\mathbf{J}_{O,k}$ is positive definite, the entire sum that builds up $\mathbf{J}_O$ is also positive definite.

Fig. 3 shows the results of applying full observability to the same monobot model as the one portrayed in Fig. 2. Note how the steady state (robot pose and landmark locations) is now unbiased with respect to the initial state estimates. Furthermore, state covariances are also smaller than those in Fig. 2.

B. External Sensor

Instead of using one of the landmarks as a global reference, one could also use a fixed sensor to measure the position of the robot, for example, by positioning a camera that observes the vehicle at all times. For such cases, the monobot measurement model may take the form

$$\begin{bmatrix} z_k^{(0)} \\ \mathbf{z}_k \end{bmatrix} = \begin{bmatrix} 1 & \mathbf{0}_{1\times n} \\ -\mathbf{1}_{n\times 1} & \mathbf{I} \end{bmatrix} \mathbf{x} + \begin{bmatrix} w_k^{(0)} \\ \mathbf{w}_k \end{bmatrix}. \tag{17}$$

The characteristics of the observability matrix, and the Fisher information matrix, are exactly the same as for the previous case. This new model is once more fully observable. The results are theoretically

equivalent to the previous case. The choice of one technique over the other would depend on the availability of such external sensor and on its measurement noise covariance characteristics.

The key point here is that we have proved that full observability, i.e., zero mean steady-state error, is indeed possible in SLAM without the need of an oracle (an external sensor) whose reading needs to be available at all times in order to preserve observability, but by simply anchoring the first observed landmark to the global reference frame.

As with any sequential innovation KF for a fully observable system, partial observability occurs until the entire set of observations spanning the state space is completed. So, if the anchor landmark is not observed for a certain period of time, the filter will be reconstructing a partially observable state estimate. But, when the anchor landmark is reobserved, the system becomes fully observable again.

Full observability however, cannot be guaranteed if the vehicle loses permanent sight of the initial anchor. Nevertheless, the effect of partial observability is precisely the steady-state error (and larger covariance) due to coupled error at the first iteration of the filter. So, in practice, full observability need only be guaranteed at the beginning of the filter.

Finally, a good strategy for any local submap approach to SLAM is to build many local maps, with one attached to each anchor needed to cover the entire mapped area. In this way, full observability will guarantee optimal vehicle and landmark localization, with the smallest possible variances for each submap.

C. Planar Vehicle

The results from the previous section are easily extensible to more complicated vehicle models, provided the linearization technique chosen is sufficiently accurate. For example, the measurement model of a global reference fixed at the origin, for the nonlinear vehicle from Section VI, is $\mathbf{h}^{(0)} = -\mathbf{R}^{\top}\mathbf{t} + \mathbf{w}^{(0)}$, and its corresponding Jacobian is

$$\mathbf{H}^{(0)} = \begin{bmatrix} -\mathbf{R}^{\top} & -\dot{\mathbf{R}}^{\top}\mathbf{t} & \mathbf{0}_{2\times 2n} \end{bmatrix}. \tag{18}$$

The external sensor case is even simpler, $\mathbf{h}^{(0)} = \mathbf{t} + \mathbf{w}^{(0)}$, and

$$\mathbf{H}^{(0)} = \begin{bmatrix} \mathbf{I} & \mathbf{0}_{2\times(2n+1)} \end{bmatrix}. \tag{19}$$

In both cases, the symbolic manipulation of (18) and (19) with a commercial algebra package, produced full rank observability matrices. That is, for the planar mobile robot platform used, only one 2-D global reference, or the use of a sensor that can measure the xy position of the robot, are sufficient to attain full observability in SLAM.

VIII. Conclusion

We have shown how partial observability hinders full reconstructibility of the state space in the KF approach to SLAM. Partial observability makes the final map dependent on the initial observations. Nevertheless, marginal stability guarantees convergence of the Riccati equation to a positive semidefinite covariance matrix. The effects of partial observability can easily be remedied either by anchoring the map to the first landmark observed or by having an external sensor that sees the vehicle at all times.

Guaranteeing full observability versus simply neglecting the steady-state error of the partially observable case has the advantage of producing smaller vehicle and landmark covariance estimates.

References

[1] H. F. Durrant-Whyte, "Uncertain geometry in robotics," *IEEE J. Robot. Autom.*, vol. 4, no. 1, pp. 23–31, Feb. 1988.

[2] R. C. Smith and P. Cheeseman, "On the representation and estimation of spatial uncertainty," *Int. J. Robot. Res.*, vol. 5, no. 4, pp. 56–68, 1986.

[3] M. W. M. G. Dissanayake, P. Newman, S. Clark, H. F. Durrant-Whyte, and M. Csorba, "A solution to the simultaneous localization and map building (SLAM) problem," *IEEE Trans. Robot. Autom.*, vol. 17, no. 3, pp. 229–241, Jun. 2001.

[4] P. M. Newman, "On the structure and solution of the simultaneous localization and map building problem," Ph.D. dissertation, Univ. of Sydney, Sydney, Australia, Mar. 1999.

[5] J. E. Guivant and E. M. Nieto, "Solving computational and memory requirements of feature-based simultaneous localization and mapping algorithms," *IEEE Trans. Robot. Autom.*, vol. 19, no. 4, pp. 749–755, Aug. 2003.

[6] P. W. Gibbens, G. M. W. M. Dissanayake, and H. F. Durrant-Whyte, "A closed form solution to the single degree of freedom simultaneous localization and map building (SLAM) problem," in *Proc. IEEE Int. Conf. Decision Control*, Sydney, Australia, Dec. 2000, pp. 408–415.

[7] S. J. Kim, "Efficient simultaneous localization and mapping algorithms using submap networks," Ph.D. dissertation, MIT, Cambridge, MA, Jun. 2004.

[8] S. J. Julier, "The stability of covariance inflation methods for SLAM," in *Proc. IEEE/RSJ Int. Conf. Intell. Robots Syst.*, Las Vegas, NV, Oct. 2003, pp. 2749–2754.

[9] Y. Bar-Shalom, X. R. Li, and T. Kirubarajan, *Estimation with Applications to Tracking and Navigation*. New York: Wiley, 2001.

[10] J. Neira and J. D. Tardós, "Data association in stochastic mapping using the joint compatibility test," *IEEE Trans. Robot. Autom.*, vol. 17, no. 6, pp. 890–897, Dec. 2001.

[11] T. Vidal-Calleja, J. Andrade-Cetto, and A. Sanfeliu, "Estimator stability analysis in SLAM," in *Proc. 5th IFAC/EURON Symp. Intell. Auton. Veh.*, Lisbon, Portugal, Jul. 2004.

[12] J. Andrade-Cetto, "Environment learning for indoor mobile robots," Ph.D. dissertation, Tech. Univ. Catalonia (UPC), Barcelona, Spain, Apr. 2003.